TM9/Phg1 and SadA proteins control surface expression and stability of SibA adhesion molecules in *Dictyostelium*

Romain Froquet, Marion le Coadic, Jackie Perrin, Nathalie Cherix, Sophie Cornillon, and Pierre Cosson
Département de Physiologie Cellulaire et Métabolisme, Centre Médical Universitaire, 1211 Geneva 4, Switzerland

ABSTRACT **TM9 proteins form a family of conserved proteins with nine transmembrane domains essential for cellular adhesion in many biological systems, but their exact role in this process remains unknown. In this study, we found that genetic inactivation of the TM9 protein Phg1A dramatically decreases the surface levels of the SibA adhesion molecule in *Dictyostelium* amoebae. This is due to a decrease in *sibA* mRNA levels, in SibA protein stability, and in SibA targeting to the cell surface. A similar phenotype was observed in cells devoid of SadA, a protein that does not belong to the TM9 family but also exhibits nine transmembrane domains and is essential for cellular adhesion. A contact site A (csA)-SibA chimeric protein comprising only the transmembrane and cytosolic domains of SibA and the extracellular domain of the *Dictyostelium* surface protein csA also showed reduced stability and relocalization to endocytic compartments in *phg1A* knockout cells. These results indicate that TM9 proteins participate in cell adhesion by controlling the levels of adhesion proteins present at the cell surface.**

Monitoring Editor
Peter Van Haastert
University of Groningen

Received: Apr 20, 2011
Revised: Dec 14, 2011
Accepted: Dec 21, 2011

INTRODUCTION

Cell–substrate adhesion is essential in many biological processes, such as development, lymphocyte migration, and metastasic dissemination (Hood and Cheresh, 2002). Attachment of phagocytic cells to particles is also necessary to allow their subsequent engulfment. In one of the best-studied examples, cell surface integrins bind to the extracellular matrix and connect it with the actin cytoskeleton and to a complex network of cytosolic proteins. This system is at play during the migration of fibroblasts in the connective tissue, as well as during integrin-dependent phagocytosis (e.g., in opsonized microorganisms) by macrophages (Cougoule *et al.*, 2004).

The amoeba *Dictyostelium discoideum* is a widely used model system for studying cellular adhesion and phagocytosis. This professional phagocyte feeds upon microorganisms in the soil, and its phagocytic machinery resembles that of mammalian phagocytes (Cosson and Soldati, 2008). Remarkably, Sib proteins, which perform as adhesion molecules in *Dictyostelium*, present features also found in mammlian integrin β chains, notably an extracellular Von Willebrandt A domain, a glycine-rich transmembrane domain, and a highly conserved cytosolic domain interacting with talin (Cornillon *et al.*, 2006). Genetic inactivation of *sibA* or *sibC* causes a partial loss of cellular adhesion to certain substrates and particles, indicating the redundant roles of these two molecules in cell adhesion (Cornillon *et al.*, 2008). Genetic analysis in *Dictyostelium* also uncovered the essential role of two additional membrane proteins in adhesion, Phg1A (Cornillon *et al.*, 2000) and SadA (Fey *et al.*, 2002). Both *phg1A* and *sadA* knockout cells are strongly defective for cellular adhesion and phagocytosis, but as detailed in this paper and elsewhere, the precise role of these proteins in cellular adhesion has yet to be elucidated.

Phg1A is a member of a family of three proteins in *Dictyostelium*, named Phg1A, -B, and -C, and characterized by the presence of nine transmembrane domains and a high degree of sequence conservation (Benghezal *et al.*, 2003). There are four related gene

This article was published online ahead of print in MBoC in Press (http://www.molbiolcell.org/cgi/doi/10.1091/mbc.E11-04-0338) on January 4, 2012.

Address correspondence to: Pierre Cosson (pierre.cosson@unige.ch).

Abbreviations used: csA, contact site A; ECL, enhanced chemiluminescence; GST, glutathione *S*-transferase; HRP, horseradish peroxidase; Ig, immunoglobulin; PBS, phosphate-buffered saline; qRT-PCR, quantitative reverse transcriptase PCR; TM9SF, transmembrane 9 superfamily.;

© 2012 Froquet *et al.* This article is distributed by The American Society for Cell Biology under license from the author(s). Two months after publication it is available to the public under an Attribution–Noncommercial–Share Alike 3.0 Unported Creative Commons License (http://creativecommons.org/licenses/by-nc-sa/3.0).
"ASCB®," "The American Society for Cell Biology®," and "Molecular Biology of the Cell®" are registered trademarks of The American Society of Cell Biology.

products in humans (TM9SF1, -2, -3, and -4), three in *Saccharomyces cerevisiae* (TMN1, -2, and -3; Froquet *et al.*, 2008), and three in *Drosophila* (Bergeret *et al.*, 2008). The term TM9SF (for transmembrane 9 superfamily) has been widely used, but such a small family of closely related gene products is more adequately described as the TM9 family. Very little is known about the function of TM9/Phg1 proteins in different organisms. Genetic inactivation of members of this family causes cell adhesion defects in organisms as distinct as *Dictyostelium* (Cornillon *et al.*, 2000), *S. cerevisiae* (Froquet *et al.*, 2008), and *Drosophila* (Bergeret *et al.*, 2008). In humans, TM9SF4 (the orthologue of Phg1A) is overexpressed in metastatic melanoma cells, in which it is essential for cannibal phagocytic activity (Lozupone *et al.*, 2009). The ability of some metastatic cells to phagocytose nonmalignant cells and to feed upon them may contribute to increased cell survival and the metastatic process (Lozupone *et al.*, 2009). Phg1A was found in endosomal compartments in *S. cerevisiae* (Singer-Kruger *et al.*, 1993) and in *Dictyostelium* (Cornillon *et al.*, 2000), as well as in human cells (Schimmoller *et al.*, 1998; Bagshaw *et al.*, 2005), but the mechanism linking Phg1 proteins to adhesion remains unelucidated to date.

The situation is even less clear for SadA (Fey *et al.*, 2002): there is no identified orthologue of this protein in non-*Dictyostelium* organisms. Like Phg1 proteins, it features a large N-terminal domain plus a C-terminal region with nine putative transmembrane domains, and could therefore be classified topologically as a TM9 protein, but it does not show any significant sequence homology with TM9/Phg1 proteins. Although genetic inactivation of SadA results in a loss of cellular adhesion, the exact role of SadA in cellular adhesion is not established.

In this study, we show that Phg1A and SadA play a role in cell adhesion in *Dictyostelium* by controlling the levels of SibA adhesion molecules at the cell surface, an effect achieved by influencing the level of *sibA* transcripts, as well as the intracellular transport and stability of the SibA protein.

RESULTS

SibA, *phg1A*, and *sadA* mutant cells exhibit similar adhesion defects

To compare the adhesion defects observed in *sibA*, *sadA*, and *phg1A* knockout cells, we measured their ability to phagocytose various particles. For this, wild-type or isogenic mutant cells were incubated in medium containing fluorescent particles (latex beads or bacteria), and the internalized material was quantified by flow cytometry. As shown previously (Cornillon *et al.*, 2000), specific defects in adhesion produce defects in phagocytosis that are limited to a subset of particles. Compared with wild-type cells, *phg1A*, *sadA*, and *sibA* mutant cells exhibited a strong defect for phagocytosis of latex beads, a more attenuated defect for phagocytosis of *Escherichia coli* bacteria, and essentially unaffected phagocytosis of *Klebsiella pneumoniae* bacteria (Figure 1). The defects observed were quantitatively less pronounced in *sibA* than in *phg1A* or *sadA* mutant cells, potentially reflecting the residual activity of SibC in *sibA* knockout cells (Cornillon *et al.*, 2008). Little or no reduction was seen in fluid-phase macropinocytosis (Figure 1), a process mechanistically similar to phagocytosis, but independent of cellular adhesion. The fact that genetic inactivation of *PHG1A* or *SADA* creates adhesion defects qualitatively similar to those observed in *sibA* knockout cells suggests that Phg1A and SadA may regulate function or expression of SibA.

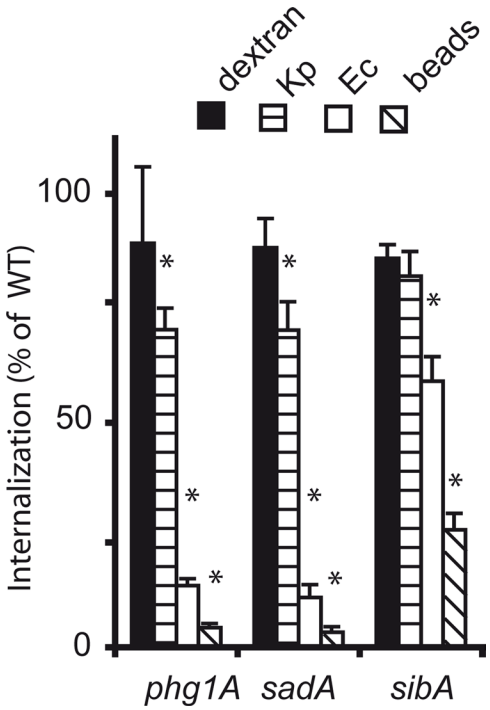

FIGURE 1: Phagocytosis defects in *phg1A*, *sadA*, and *sibA* knockout cells. Wild-type or mutant *Dictyostelium* cells were incubated for 20 min in HL5 medium containing either fluorescent phagocytic particles (latex beads [beads], *K. pneumoniae* [Kp], or *E. coli* [Ec] bacteria) or a fluorescent fluid-phase marker (dextran). The internalized fluorescence was analyzed by flow cytometry and expressed as a percentage of internalization in wild-type cells. Qualitatively, *phg1A*, *sadA*, and *sibA* mutants presented similar phenotypes compared with wild-type cells: virtually normal uptake of fluid phase and of *K. pneumoniae*, diminished phagocytosis of *E. coli*, and minimal phagocytosis of latex beads. The average and SEM of at least four experiments are indicated. *, significantly different from wild-type ($p < 0.05$ with Student's *t* test).

Phg1A and SadA control surface levels of SibA

To assess the possible involvement of Phg1A and SadA in controlling surface levels of SibA, we biotinylated the surface of wild-type or mutant cells, immunoprecipitated SibA, and revealed it with horseradish peroxidase (HRP)-coupled avidin. As in *sibA* knockout cells, SibA was virtually absent from the surface of *phg1A* and *sadA* knockout cells (Figure 2A). The surface levels of SibA were not significantly affected in *talin* or *phg2* mutant cells compared with wild-type cells (Figure 2A).

To assess the total amount of SibA, we used gel electrophoresis to separate whole-cell lysates, transferred them to nitrocellulose, and revealed SibA with anti-SibA antibodies. The total amount of SibA in both *phg1A* and *sadA* mutant cells was significantly reduced compared with wild-type cells, whereas only relatively minor differences were seen in *talin* or *phg2* mutant cells (Figure 2B). These results suggest the absence of SibA from the surface of *phg1A* and *sadA* mutant cells is at least partly due to a decrease in the total amount of cellular SibA. In addition, the SibA surface-to-total ratio was markedly lower in *phg1A* and in *sadA* mutant cells (0.27 and 0.0, respectively) than in wild-type cells (1.0), suggesting the intracellular distribution of SibA may be affected in *phg1A* and *sadA* mutant cells.

To further test whether loss of SibA accounted for the adhesion defect observed in *phg1A* mutant cells, we assessed the effect of temperature on cellular levels of SibA. Previous experiments have shown that the adhesion defect of *phg1A* mutant cells is significantly increased at 26°C compared with 20°C (Benghezal *et al.*,

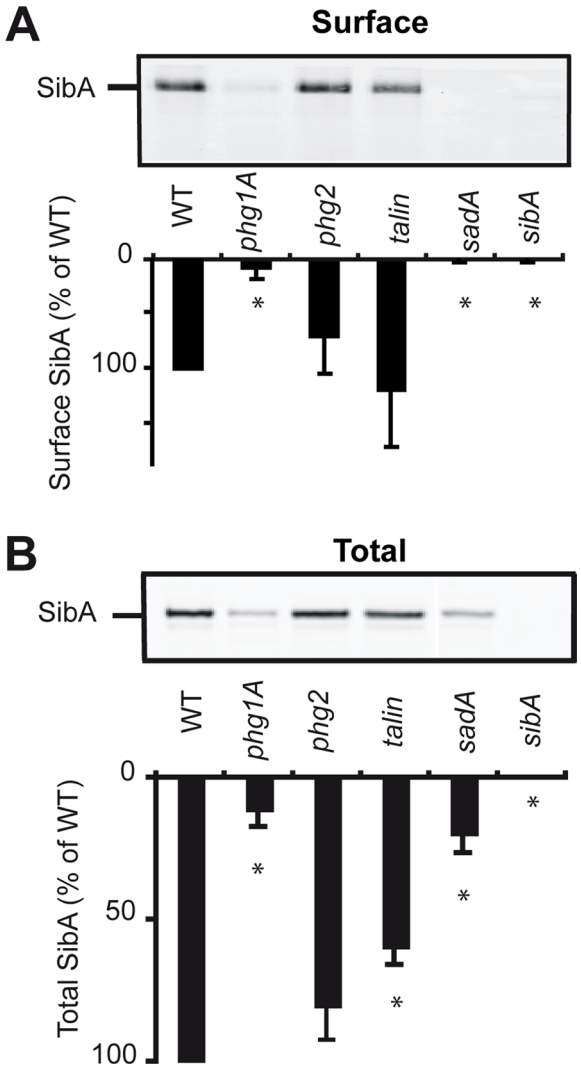

FIGURE 2: Phg1A and SadA control surface expression of SibA. (A) To assess the presence of SibA at the cell surface, we surface-biotinylated and then lysed wild-type and mutant cells. SibA was purified by immunoprecipitation, migrated on a 7% polyacrylamide gel, and revealed with HRP-coupled avidin. While SibA was readily detectable at the surface of wild-type, *talin*, or *phg2* cells, it was virtually absent from the surface of *sibA*, *phg1A*, and *sadA* mutant cells. (B) To determine the total cellular amount of SibA, we separated cellular proteins by electrophoresis and revealed SibA with a specific antibody. (lane 10): The amount of SibA was quantified and expressed as the percentage of the amount observed in wild-type cells. The average and SEM of four independent experiments are indicated. *, significantly different from wild-type ($p < 0.05$ with Student's *t* test).

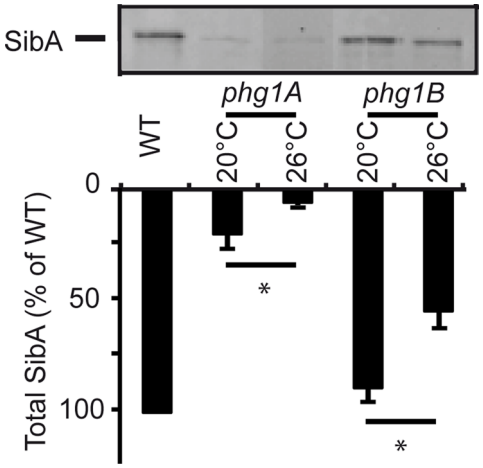

FIGURE 3: Phg1A and Phg1B control cellular levels of SibA in a temperature-dependent manner. Wild-type or mutant (*phg1A* or *phg1B*) cells were grown at the indicated temperature for 24 h. The total cellular amount of SibA was determined by Western blot, as described in the legend to Figure 2. The average and SEM of four independent experiments are indicated. *, significantly different from wild-type ($p < 0.05$ with Student's *t* test).

2003). We observed that the levels of SibA were indeed significantly lower at 26°C than at 20°C (Figure 3). It was also shown previously that *phg1B* mutant cells exhibit a (modest) adhesion defect only at 26°C. In agreement with this, cellular levels of SibA in *phg1B* mutant cells were not affected at 20°C, but were significantly lower at 26°C (Figure 3).

Phg1A and SadA control production and stability of SibA

Decreased cellular levels of SibA could be due to a decrease in its production, to an increased turnover, or to a combination of both. To evaluate these two possibilities, we first measured by quantitative reverse transcriptase PCR (qRT-PCR) the level of *sibA* mRNA in various cell lines to provide an indication of *sibA* mRNA expression level. We observed a statistically significant decrease in the amount of *sibA* mRNA in *phg1A* mutant cells relative to wild-type cells (37% of wild-type level) (Figure 4). Less prominent and not statistically significant alterations in *sibA* mRNA levels were observed in *sadA* mutant cells (72% of wild-type, $p > 0.1$) and in other mutant cells analyzed (Figure 4).

To measure the stability of the SibA protein, we incubated cells in the presence of cycloheximide to inhibit protein synthesis. At various times, aliquots of the cells were collected, and the remaining SibA was revealed by immunoblotting (Figure 5). In wild-type cells, SibA was relatively stable (70% remaining after 2 h of chase). In contrast, SibA was more rapidly degraded in *phg1A* mutant cells, and even more so in *sadA* mutant cells (37 and 13% remaining after 2 h of chase, respectively; Figure 5).

These results indicate that Phg1A and SadA control the total cellular amount of SibA by influencing its turnover and, at least in the case of Phg1A, its production.

Phg1A controls the sorting of SibA in the endocytic pathway

The decreased stability of SibA in *phg1A* and *sadA* mutant cells may be indicative of perturbed intracellular targeting. Endogenous SibA is present in such relatively small amounts in *Dictyostelium* cells that it is not detectable by immunofluorescence. To circumvent this limitation, we constructed a plasmid encoding a chimeric protein (csA-SibA) composed of the extracellular domain of the *Dictyostelium* adhesion molecule contact site A (csA) linked to the transmembrane and cytosolic domains of SibA (Figure 6A). We then introduced this plasmid in wild-type or *phg1A* mutant cells. *SadA* mutant cells were not analyzed further in this study, because they proved difficult to grow and to transfect, due to marked defects in their actin cytoskeleton (Fey *et al.*, 2002).

As a control, we constructed and expressed in wild-type and *phg1A* knockout cells a second chimeric csA protein anchored in the membrane by a classical 21-amino acid hydrophobic transmembrane domain followed by a very short cytosolic domain (csA-TM; Figure 6A).

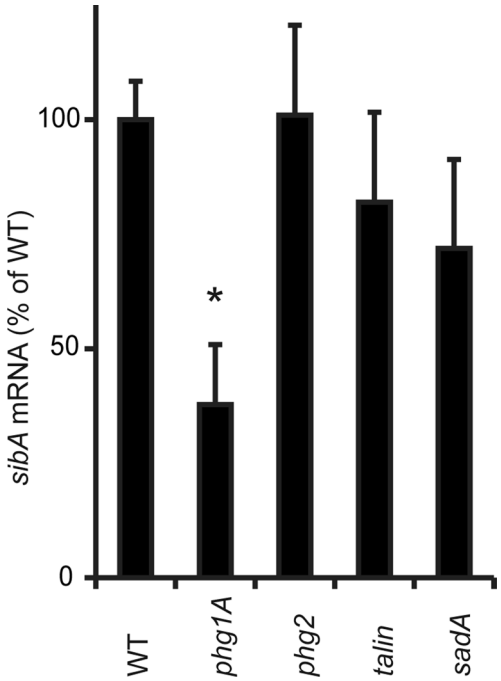

FIGURE 4: *SibA* mRNA levels are decreased in *phg1A* mutant cells. The amount of *sibA* mRNA was determined in mutant cells by RT-PCR and expressed as a percentage of the level measured in wild-type cells. The average and SEM of three independent experiments are indicated. *, significantly different from wild-type ($p < 0.05$ with Student's *t* test).

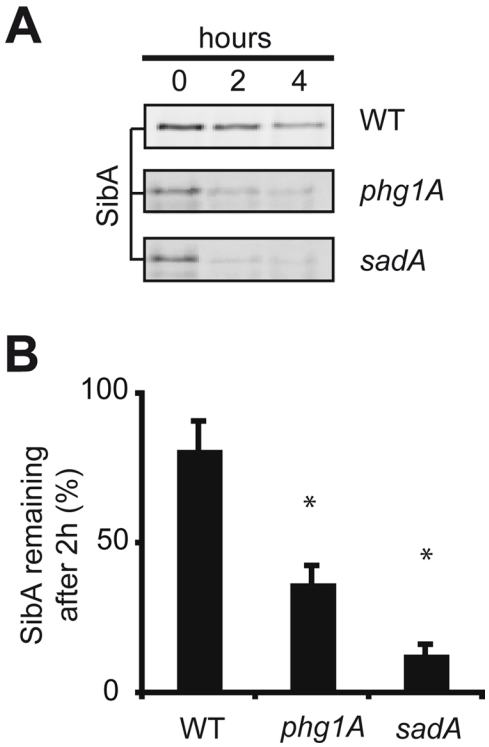

FIGURE 5: The SibA protein is less stable in *phg1A* and *sadA* mutant cells than in wild-type cells. (A) Wild-type and mutant cells were incubated in the presence of cycloheximide for 0, 2, or 4 h and then lysed; the remaining SibA was detected by Western blotting after gel electrophoresis. To obtain equivalent signals at time zero, 10^6 cells were loaded per lane for *phg1A* and *sadA* mutant cells and 10^5 for wild-type cells. (B) The signals were quantified to determine the percentage of SibA remaining after 2 h of chase. The average and SEM of six independent experiments are indicated. *, significantly different from wild-type ($p < 0.05$ with Student's *t* test).

csA-SibA was detected by immunofluorescence at the cell surface, as well as in intracellular compartments in wild-type cells (Figure 6B). In contrast, surface csA-SibA was undetectable in *phg1A* mutant cells (Figure 6B). To confirm this result in a more quantitative manner, we analyzed labeled cells by flow cytometry to simultaneously measure the levels of csA protein at the surface and inside individual cells. This analysis confirmed that *phg1A* knockout cells presented at their surface a much smaller portion of total csA-SibA than wild-type cells (Figure 6C). We observed a very similar behavior for a csA-SibC chimera in which the csA extracellular domain was fused to the transmembrane and cytosolic domains of SibC: a greater amount was expressed at the surface of wild-type than of *phg1A* mutant cells (respectively: 81 ± 19 and 18 ± 2; n = 6; p = 0.04). In contrast, csA-TM was expressed at similar levels at the surface of both cell types (Figure 6D).

Finally, like SibA, csA-SibA was less stable in *phg1A* mutant cells than in wild-type cells, as revealed by chase experiments in the presence of cycloheximide (Figure 6E). Taken together these results indicate that csA-SibA, like SibA, is excluded from the cell surface and presumably targeted for intracellular degradation in *phg1A* mutant cells.

To determine where *phg1A*-dependent intracellular sorting occurred, we assessed with immunofluorescence the localization of the csA-SibA chimera in wild-type and in *phg1A* mutant cells (Figure 7). We detected csA-SibA in small compartments in both cell types, sometimes grouped in a juxtanuclear region, a disposition reminiscent of previously characterized early endocytic compartments (Charette *et al.*, 2006). Indeed, all compartments containing csA-SibA also contained p25, a marker present at the cell surface, as well as in early and recycling endosomes in *Dictyostelium* (Charette *et al.*, 2006; Figure 7, A and B). However, some of the p25-positive compartments did not contain detectable levels of csA-SibA, suggesting csA-SibA was restricted to a subpopulation of early and recycling endosomes. CsA-SibA was not detected in more mature lysosomal compartments labeled with an anti-p80 antibody in either wild-type (Figure 7C) or *phg1A* mutant cells (unpublished data). As shown previously, p80 is present at the cell surface and in lysosomes, but virtually absent from recycling endosomes (Ravanel *et al.*, 2001). Note that in these experiments, permeabilization resulted in weaker cell surface staining not readily detectable by immunofluorescence. These experiments indicate that in both wild-type and *phg1A* knockout cells, csA-SibA is present at the cell surface and in early endocytic compartments, but that cell surface levels of csA-SibA are much lower in *phg1A* knockout cells than in wild-type cells.

Absence of SibA-associated proteins

Phg1A may control the sorting and stability of SibA via direct interactions or via a more general effect on sorting and transport in the endocytic pathway. To distinguish between these two possibilities, we designed two distinct experiments to detect direct interaction between Phg1A and SibA. First, we labeled cell surface proteins with biotin, lysed the cells, immunoprecipitated SibA, and probed for coprecipitated biotinylated proteins with HRP-coupled avidin (Figure 8A). No associated proteins were detected, which suggests that there may not be a stable association of SibA with another chain (equivalent to the α chain of integrins) or with Phg1A or SadA. This method, however, would not detect an association of Phg1A with

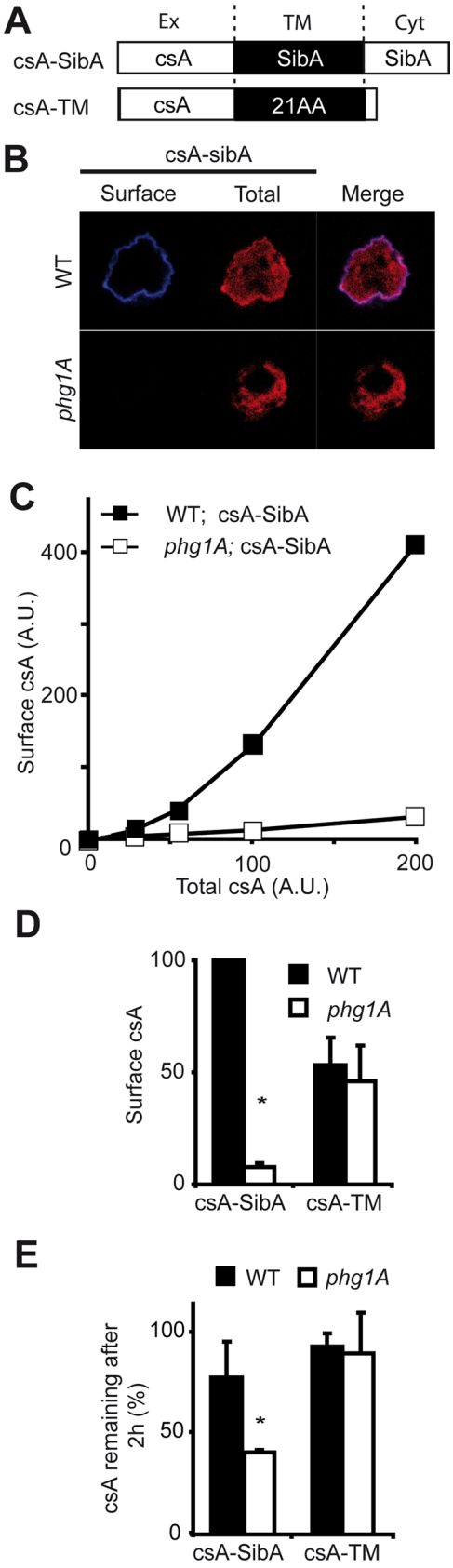

FIGURE 6: Intracellular sequestration of csA-SibA in *phg1A* mutant cells. (A) A chimeric protein comprising the csA extracellular domain fused to the transmembrane and cytosolic domains of SibA (csA-SibA) was expressed in wild-type and in *phg1A* mutant cells. As a control, a csA protein fused to a classical hydrophobic transmembrane domain was used (csA-TM). (B) csA-SibA was labeled by immunofluorescence before (Surface, blue) and after (Total, red) permeabilization in transfected wild-type and *phg1A* mutant cells, using an antibody specific for the csA extracellular domain. The pictures presented were obtained with a confocal microscope in consecutive sequence and with identical settings. (C) The surface and total csA was labeled as described in (B) for wild-type and *phg1A* mutant cells expressing csA-SibA. The fluorescence was quantified by flow cytometry. (D) The average and SEM of seven independent flow cytometry experiments (described in C) are represented in this bar graph. The surface csA value used was that corresponding to a total csA expression of 200 in (C). (E) Stability of csA-SibA and csA-TM in wild-type and *phg1A* mutant cells. The stability of the protein was determined during a chase in the presence of cycloheximide, as described in the legend to Figure 5. CsA-SibA was less stable in *phg1A* mutant cells than in wild-type cells, while the stability of csA-TM was comparable in both cells. The average and SEM of four independent experiments are indicated. *, significantly different from wild-type ($p < 0.05$ with Student's *t* test).

SibA occurring in an intracellular compartment. Therefore, in a second experiment, we used cells expressing Phg1A tagged with a glutathione *S*-transferase (GST) at its C-terminus, a fusion protein that was shown previously to fully complement the defects of a *phg1A* mutant cell (Benghezal *et al.*, 2003). We then purified Phg1A-GST using a glutathione-coupled resin, and attempted to detect associated SibA by Western blotting (Figure 8B). We did not detect any SibA coprecipitated with Phg1A-GST, even when material precipitated from 30×10^6 cells was loaded on a single lane. Although these results suggest that the Phg1A and SibA proteins do not associate stably in living cells, they do not rule out a transient or an unstable interaction between these two proteins.

DISCUSSION

The results presented in this study indicate that Phg1A and SadA participate in cellular adhesion by controlling the levels of SibA adhesion molecules present at the cell surface. Phg1A and SadA achieve this effect by controlling to various extents the levels of *sibA* mRNA, the stability of the SibA protein, and its targeting to the cell surface. In the absence of Phg1A, SibA is less abundantly produced, less stable, and excluded from the cell surface. A similar pattern is observed in *sadA* mutant cells, in which the stability and surface targeting of SibA are strongly defective. By establishing connections among Phg1A, SadA, and SibA, these results provide a more complete picture of the adhesion machinery in *Dictyostelium*, one that is centered on the function of SibA adhesion molecules. Indeed, the major gene products shown to be essential for efficient adhesion now have a clear link with SibA: talin and myosin VII form a complex (Gebbie *et al.*, 2004; Tuxworth *et al.*, 2005) that binds the cytosolic domain of SibA (Cornillon *et al.*, 2006), while Phg1A and SadA control expression of SibA at the cell surface (this study).

It is surprising to observe that genetic inactivation of *sadA* or *phg1A* would yield such similar phenotypes in mutant cells, since the corresponding proteins show no clear homology. On the other hand, both proteins share the same general topology with a large N-terminal extracellular domain and nine C-terminal transmembrane domains. Although the classical definition of TM9 proteins, based on sequence conservation (Schimmoller *et al.*, 1998), would not include SadA, it is possible that more subtle structural features are conserved between Phg1A and SadA proteins. A more advanced knowledge of the structure and function of TM9 proteins may allow us in the future to delineate an extended TM9

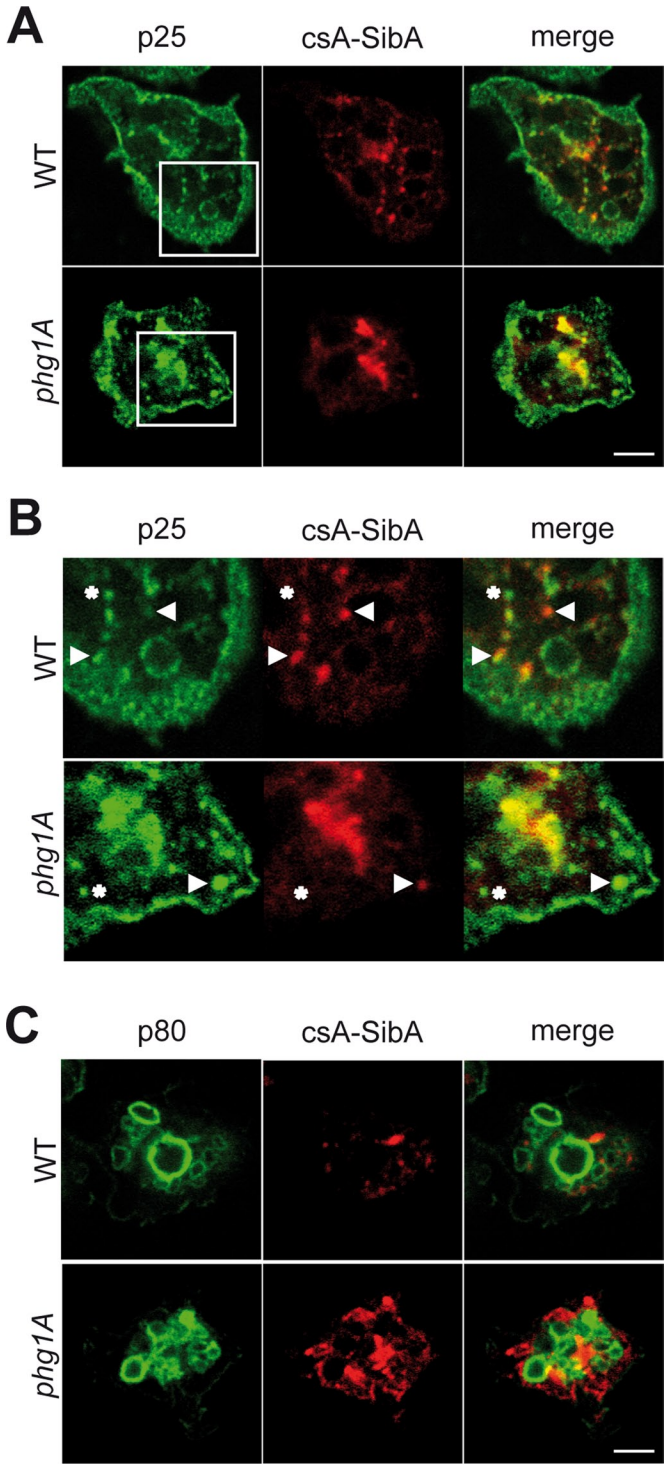

FIGURE 7: Intracellular csA-SibA is localized in early endocytic compartments. Wild-type and *phg1A* mutant cells expressing csA-SibA were fixed and permeabilized, and intracellular csA-SibA was detected with a rabbit antibody recognizing the SibA cytosolic domain, and a fluorescent secondary antibody (red). In the same cells, p25 (A and B) or p80 (C) were detected with specific mouse antibodies (green). (B) An enlarged portion of (A). In both wild-type and *phg1A* cells, csA-SibA was present in intracellular compartments positive for p25 (arrowheads) but not for p80. Some p25-positive compartments did not contain csA-SibA (asterisks), suggesting that csA-SibA is sorted differently from p25 in the early endocytic pathway. Note that in these experiments, surface csA-SibA is difficult to detect due to cell permeabilization.

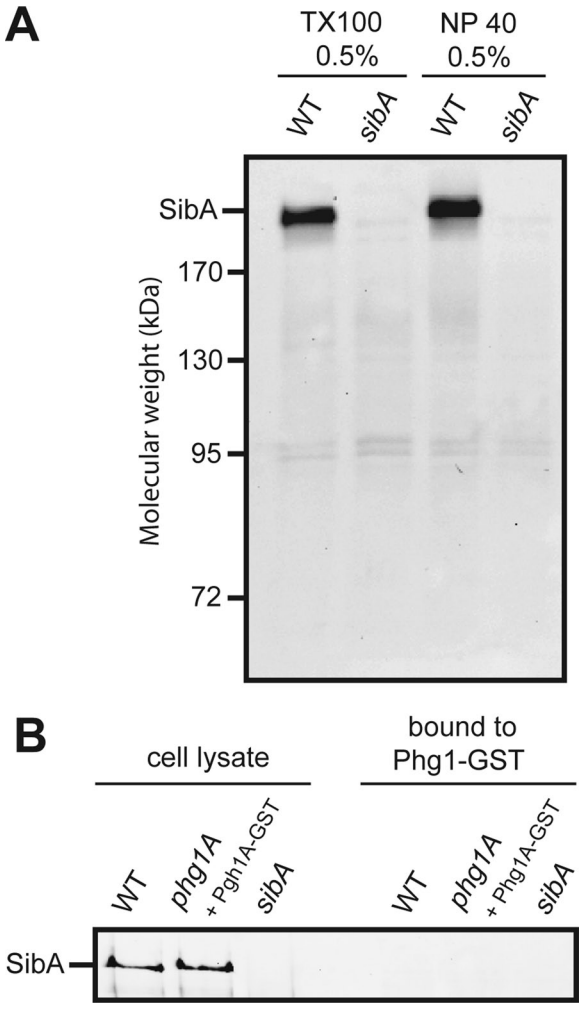

FIGURE 8: No detectable association between Phg1A and SibA. (A) Cell surface proteins were biotinylated in wild-type or *sibA* mutant cells. Cells were lysed in the presence of either Triton X-100 or Nonidet P40, and SibA was immunoprecipitated. Proteins precipitated from 10^7 cells were separated on a polyacrylamide gel and revealed with HRP-coupled avidin. No protein specifically coprecipitating with SibA was detected. (B) Phg1A-GST was expressed in *phg1A* mutant cells and precipitated in the presence of 0.5% Triton X-100. The proteins were separated by electrophoresis and SibA was revealed with a specific antibody. As a control, wild-type or sibA cells were used. Cellular lysates (0.5×10^6 cells), as well as precipitated samples (10^7 cells), were analyzed. No detectable SibA was coprecipitated with Phg1A-GST.

superfamily that would include SadA and possibly other proteins. As our knowledge of TM9 proteins increases, we will presumably discover whether the structural and functional similarities between SadA and Phg1A are significant or merely coincidental.

The overall organization of the adhesion machinery in *Dictyostelium* and in mammalian cells is remarkably similar. SibA proteins and integrin β chains also share a number of structural and functional features (Cornillon *et al.*, 2006). It is thus tempting to speculate that TM9 proteins in mammalian cells may also control surface expression of proteins involved in cellular adhesion, particularly integrins. In addition, Phg1A has also been implicated in the control of adhesion in yeast cells (Froquet *et al.*, 2008) and *Drosophila* phagocytic cells (Bergeret *et al.*, 2008), which use very different sets of adhesion molecules. We speculate that a connection will be established

between TM9/Phg1 proteins and surface expression of key adhesion molecules in these various systems.

MATERIALS AND METHODS

Cell culture and mutant cells

D. discoideum strains were grown in HL5 medium at 23°C and subcultured twice a week to maintain a maximal density of 10^6 cells/ml. All mutant strains used in this study were derived from the subclone DH1–10 (Cornillon *et al.*, 2000) of the parental axenic *Dictyostelium* strain DH1 (Caterina *et al.*, 1994). For simplicity, DH1–10 cells are referred to as wild-type cells. The *phg1A* (Cornillon *et al.*, 2000), *sibA* (Cornillon *et al.*, 2006), and *talin* (Gebbie *et al.*, 2004) mutant strains have been described previously. The *sadA* knockout mutants were generated by using the knockout plasmids previously described (Fey *et al.*, 2002). In addition to their adhesion defects, *sadA* knockout mutants presented a huge cytokinesis defect (unpublished data), as described previously (Fey *et al.*, 2002).

Expression of csA chimera

The extracellular domain of csA was amplified from genomic DNA using the two following oligonucleotides: GATACAGTTAACAAAATGAAATTTTTATTAGTATTGATAATATTATA and CTTTTCGGTACCAGTTTCTTCTGGTGTGCTGGTTG. The PCR fragment was digested with *Hpa*I and *Kpn*I and cloned into prepSC3 (a pDXA-3C plasmid with a modified *Hin*dIII-*Hpa*I-*Kpn*I-*Not*I-*Xba*I multiple-cloning site [Manstein *et al.*, 1995]) digested with *Hpa*I-*Kpn*I, creating the csA-0 intermediate construct. The csA-TM construct was obtained by amplifying the sequence coding for the transmembrane domain of CD1b-TM3 (21 aa; Mercanti *et al.*, 2010) and subcloning it in csA-0, using the *Kpn*I and *Xba*I sites. The amino acid sequence of the transmembrane domain of csA-TM is: ESDSIVLAIIVPSLLLLLCLALLWYMRRRSM.

To construct csA-SibA, we amplified the transmembrane and cytoplasmic domains of SibA (from Tyr-1850 to stop codon) by PCR and cloned them into csA-0.

Internalization assays

Phagocytosis and fluid-phase uptake were determined by shaking the cells for 20 min at 21°C in HL5 medium with either 1-µm-diameter Fluoresbrite YG carboxylate microspheres (Polysciences, Warrington, PA), rhodamine-labeled *K. pneumoniae* (Cornillon *et al.*, 2000), rhodamine-labeled *E. coli*, or 10 µg/ml of Alexa Fluor 647–labeled dextran (Molecular Probes, Eugene, OR), and measuring the internalized fluorescence in a fluorescence-activated cell sorter (FACSCalibur, Becton Dickinson, San Jose, CA) after two washes with HL5 containing 0.1% sodium azide, as described previously (Cornillon *et al.*, 2000).

Western blot analysis

To detect SibA at the cell surface, we cooled cells to 4°C and then pelleted and washed them twice with ice-cold phosphate-buffered saline (PBS; pH 7.3). The cells were then resuspended and incubated for 30 min in ice-cold PBS containing 0.25 mg/ml sulfo-succinimido-biotin (Molecular Biosciences, Boulder, CO), washed twice with ice-cold PBS containing 40 mM NH_4Cl, and then lysed on ice for 15 min in lysis buffer (PBS, 0.5% Triton X-100, 5 mg/ml iodoacetamide, 100 µm phenylmethylsulfonylfluoride, 1.5 µM aprotinin, and 47 µM leupeptin). After the nuclei were pelleted (9300 × *g* at 4°C for 5 min), the supernatant was first incubated for 15 min with protein G Sepharose beads (GE Healthcare, Sweden) and then for 1 h in the presence of a polyclonal anti-SibA antibody (Cornillon *et al.*, 2006) coupled to protein G Sepharose. Beads were washed five times with PBS containing 0.1% Triton X-100 and resuspended in sample buffer (0.103 g/ml sucrose, 5×10^{-2} M Tris, pH 6.8, 5×10^{-3} M EDTA, 0.5 mg/ml bromophenol blue, 2% SDS). Biotinylated proteins were separated on a 7% polyacrylamide gel, incubated with HRP-coupled avidin (Bio-Rad, Hercules, CA), and revealed by enhanced chemiluminescence (ECL; Amersham Biosciences, GE Healthcare, Waukesha, WI).

To determine the total amount of cellular SibA, we resuspended cell pellets in sample buffer and separated the proteins on a 7% polyacrylamide gel, after which they were transferred to a nitrocellulose membrane (Invitrogen, Carlsbad, CA). The membranes were incubated with a polyclonal anti-SibA antibody (Cornillon *et al.*, 2006) and then with an HRP-coupled donkey anti-rabbit immunoglobulin (Ig) G (Bio-Rad), washed, and revealed by ECL (Amersham Biosciences). The amount of both surface and total cellular SibA protein was evaluated using Quantity One software (Bio-Rad). As a control, serial dilutions of the wild-type sample confirmed the existence of a linear relationship between the measured signal and the amount of protein (unpublished data). Nitrocellulose membranes were stained with Ponceau red to ascertain that similar amounts of proteins were loaded in each lane.

To measure the stability of SibA or csA-SibA proteins, we incubated 2×10^6 *Dictyostelium* cells for 0, 2, or 4 h in 2 ml HL5 containing 2 mM cycloheximide. At each time point, an aliquot of the cells was collected, pelleted, and resuspended in sample buffer, and the total amount of cellular SibA was revealed by Western blotting, as described above. To obtain equivalent signals at time zero, 10 times more cells were loaded per lane for *phg1A* and *sadA* mutant cells than for wild-type cells (10^6 vs. 10^5 cells per lane, respectively).

Real-time PCR

As described previously (Cornillon *et al.*, 2008), wild-type or mutant cells were grown in HL5 medium for 3 d to a final density of 10^6 cells/ml. The cells were harvested, RNAs were purified with a NucleoSpin RNA II kit (Macherey-Nagel, Duren, Germany), and real-time PCR was performed using *sibA*-specific oligonucleotides (forward: 5′-CCAACTCCGACAGATGGTTCTC-3′; reverse: 5′-AAAGAATTTGTTTTGTTTACTTCATATGCA-3′). Raw Ct values obtained with SDS 2.2 (Applied Biosystems, Bedford, MA) were imported into Excel (Microsoft, Redmond, WA), and normalization factors and fold changes were calculated. The Ig7 gene (mitochondrial large-subunit rRNA) was used to normalize PCRs. The background measured in *sibA* knockout cells was subtracted from all other results.

Immunofluorescence

To localize intracellular csA-sibA, we performed immunofluorescence on cells attached to glass coverslips. To elicit efficient adhesion of wild-type and *phg1A* cells, we allowed cells to adhere for 10 min to coverslips in phosphate buffer (2 mM Na_2HPO_4, 14.7 mM KH_2PO_4, pH 6.0, supplemented with 0.5% HL5, 100 mM sorbitol, and 100 µM $CaCl_2$). This buffer preserves the morphology of endocytic compartments (Smith *et al.*, 2010), while allowing cells to attach to their substrate in a Phg1A-independent manner (Gebbie *et al.*, 2004). We then performed immunofluorescence on fixed cells as previously described (Mercanti *et al.*, 2006), using a rabbit anti-SibA to detect csA-SibA (Cornillon *et al.*, 2006) and a mouse anti-p25 (H72) to detect p25 (Charette *et al.*, 2006).

To detect csA-TM or csA-SibA by surface immunofluorescence in unfixed cells, we used a mouse monoclonal antibody (41-71-21) directed to the csA extracellular domain (Bertholdt *et al.*, 1985). Since incubations at 4°C were found to affect cell morphology, the cell surface was labeled with this antibody for 1 min at room temperature.

Cells were then rinsed twice rapidly and fixed with 4% paraformaldehyde in 100 mM phosphate buffer (pH 7.4), incubated with an anti-mouse antibody coupled to Alexa Fluor 647, and permeabilized with methanol at −20°C. Permeabilized cells were then further incubated sequentially with anti-csA antibody and a rhodamine-coupled anti-mouse antibody to reveal intracellular csA. Cells were observed with a LSM 510 Zeiss confocal microscope (Jena, Germany). Alternatively, levels of csA-sibA and csA-TM at the cell surface and inside the cell were measured by flow cytometry (FACSCalibur) after the cells were detached from coverslips.

Coprecipitation experiments

To detect proteins associated with SibA at the cell surface, we biotinylated proteins present at the cell surface, as described in *Western blot analysis*. After lysis and immunoprecipitation of SibA, the material precipitated from 10^7 cells was loaded on each lane of an 8% polyacrylamide gel. After transfer to a nitrocellulose membrane, HRP-coupled avidin was used to reveal proteins coprecipitated with SibA.

In another attempt to detect an association of Phg1A and intracellular SibA, we expressed Phg1A-GST in *phg1A* mutant cells and purified it on glutathione beads after cell lysis, as previously described (Benghezal *et al.*, 2006). Proteins precipitated from 10^7 cells were separated on an 8% polyacrylamide gel and SibA was revealed by Western blotting, as described in *Western blot analysis*.

ACKNOWLEDGMENTS

This work was supported by grants from the Swiss National Science Foundation (31003A-135789 to P.C.) and from the Doerenkamp-Zbinden and the FENRIV foundations. We thank Prashant Nair for his participation in the initial experiments and Thierry Soldati and Oliver Hartley for critical reading of the manuscript.

REFERENCES

Bagshaw RD, Mahuran DJ, Callahan JW (2005). A proteomic analysis of lysosomal integral membrane proteins reveals the diverse composition of the organelle. Mol Cell Proteomics 4, 133–143.

Benghezal M, Cornillon S, Gebbie L, Alibaud L, Bruckert F, Letourneur F, Cosson P (2003). Synergistic control of cellular adhesion by transmembrane 9 proteins. Mol Biol Cell 14, 2890–2899.

Benghezal M *et al.* (2006). Specific host genes required for the killing of *Klebsiella* bacteria by phagocytes. Cell Microbiol 8, 139–148.

Bergeret E, Perrin J, Williams M, Grunwald D, Engel E, Thevenon D, Taillebourg E, Bruckert F, Cosson P, Fauvarque MO (2008). TM9SF4 is required for *Drosophila* cellular immunity via cell adhesion and phagocytosis. J Cell Sci 121, 3325–3334.

Bertholdt G, Stadler J, Bozzaro S, Fichtner B, Gerisch G (1985). Carbohydrate and other epitopes of the contact site A glycoprotein of *Dictyostelium discoideum* as characterized by monoclonal antibodies. Cell Differ 16, 187–202.

Caterina MJ, Milne JL, Devreotes PN (1994). Mutation of the third intracellular loop of the cAMP receptor, *cAR1*, of *Dictyostelium* yields mutants impaired in multiple signaling pathways. J Biol Chem 269, 1523–1532.

Charette SJ, Mercanti V, Letourneur F, Bennett N, Cosson P (2006). A role for adaptor protein-3 complex in the organization of the endocytic pathway in *Dictyostelium*. Traffic 7, 1528–1538.

Cornillon S, Froquet R, Cosson P (2008). Involvement of Sib proteins in the regulation of cellular adhesion in *Dictyostelium discoideum*. Eukaryot Cell 7, 1600–1605.

Cornillon S, Gebbie L, Benghezal M, Nair P, Keller S, Wehrle-Haller B, Charette SJ, Bruckert F, Letourneur F, Cosson P (2006). An adhesion molecule in free-living *Dictyostelium* amoebae with integrin β features. EMBO Rep 7, 617–621.

Cornillon S, Pech E, Benghezal M, Ravanel K, Gaynor E, Letourneur F, Bruckert F, Cosson P (2000). Phg1p is a nine-transmembrane protein superfamily member involved in *Dictyostelium* adhesion and phagocytosis. J Biol Chem 275, 34287–34292.

Cosson P, Soldati T (2008). Eat, kill or die: when amoeba meets bacteria. Curr Opin Microbiol 11, 271–276.

Cougoule C, Wiedemann A, Lim J, Caron E (2004). Phagocytosis, an alternative model system for the study of cell adhesion. Semin Cell Dev Biol 15, 679–689.

Fey P, Stephens S, Titus MA, Chisholm RL (2002). SadA, a novel adhesion receptor in *Dictyostelium*. J Cell Biol 159, 1109–1119.

Froquet R, Cherix N, Birke R, Benghezal M, Cameroni E, Letourneur F, Mosch HU, De Virgilio C, Cosson P (2008). Control of cellular physiology by TM9 proteins in yeast and *Dictyostelium*. J Biol Chem 283, 6764–6772.

Gebbie L *et al.* (2004). Phg2, a kinase involved in adhesion and focal site modeling in *Dictyostelium*. Mol Biol Cell 15, 3915–3925.

Hood JD, Cheresh DA (2002). Role of integrins in cell invasion and migration. Nat Rev Cancer 2, 91–100.

Lozupone F *et al.* (2009). The human homologue of *Dictyostelium discoideum* phg1A is expressed by human metastatic melanoma cells. EMBO Rep 10, 1348–1354.

Manstein DJ, Schuster HP, Morandini P, Hunt DM (1995). Cloning vectors for the production of proteins in *Dictyostelium discoideum*. Gene 162, 129–134.

Mercanti V, Charette SJ, Bennett N, Ryckewaert JJ, Letourneur F, Cosson P (2006). Selective membrane exclusion in phagocytic and macropinocytic cups. J Cell Sci 119, 4079–4087.

Mercanti V, Marchetti A, Lelong E, Perez F, Orci L, Cosson P (2010). Transmembrane domains control exclusion of membrane proteins from clathrin-coated pits. J Cell Sci 123, 3329–3335.

Ravanel K, de Chassey B, Cornillon S, Benghezal M, Zulianello L, Gebbie L, Letourneur F, Cosson P (2001). Membrane sorting in the endocytic and phagocytic pathway of *Dictyostelium discoideum*. Eur J Cell Biol 80, 754–764.

Schimmoller F, Diaz E, Muhlbauer B, Pfeffer SR (1998). Characterization of a 76 kDa endosomal, multispanning membrane protein that is highly conserved throughout evolution. Gene 216, 311–318.

Singer-Kruger B, Frank R, Crausaz F, Riezman H (1993). Partial purification and characterization of early and late endosomes from yeastIdentification of four novel proteins. J Biol Chem 268, 14376–14386.

Smith EW, Lima WC, Charette SJ, Cosson P (2010). Effect of starvation on the endocytic pathway in *Dictyostelium* cells. Eukaryot Cell 9, 387–392.

Tuxworth RI, Stephens S, Ryan ZC, Titus MA (2005). Identification of a myosin VII-talin complex. J Biol Chem 280, 26557–26564.